Some Applications of Lorentz Oscillator Model

Vishwamittar

Retired from Department of Physics, Panjab University, Chandigarh – 160014.
Contact Address: #121, Sector-16, Panchkula – 134113 (Haryana).
email address: vm121@hotmail.com

** The article is dedicated with immense reverence to late Nana ji (Sh. Bhagwan Das Ji), late Taya Ji (Sh. Jai Dayal Ji & Sh. Chetananand Ji), late phoopha Ji (Sh. Issar Das Ji) and late Maan Ji (Smt. Lachhmi Devi Ji).*

Submitted on 27-01-2023

Abstract

This article is devoted to the description of the Lorentz oscillator model, which refers to the classical concept that electrons in an atom behave as forced damped harmonic oscillators under the influence of an oscillating electric field. This idea has been used to derive expressions for complex dielectric function, complex refractive index and normal incidence reflectivity and their detailed analysis. These quantities have also been discussed for the Drude model for metals, which can be considered as a special case of the Lorentz model. Some typical applications of these models and their combination have also been dealt with. The fascinating thing about these models is that despite being classical in nature they lead to reasonably reliable results for otherwise quantum mechanical systems. An effort has been made to present the material in a pedagogical manner so that it can be easily followed by undergraduate students.

1 Introduction

The 1902 physics Nobel laureate Lorentz (July 18,1853 – Feb. 4, 1928) became a cynosure in the history of physics by 'completing what was left unfinished by his predecessors and preparing the ground for the fruitful reception of new ideas based on the quantum theory' [1]. His outstanding contributions are refinement of Maxwell's electromagnetic theory including works in optics; general theory of electrical and optical phenomena of moving bodies; derivation of Lorentz force law which describes dynamics of a charged particle in the presence of electric and magnetic fields; insightful conceptualization of electron, its mathematical theory and use to explain Zeeman effect (the splitting of atomic spectral lines in the presence of magnetic field); and ingenious idea of local time and derivation of Lorentz transformations (which can be used to calculate the earlier proposed
Lorentz-Fitzgerald length contraction) that constitute the natural outcome of Einstein's special theory of relativity. Even before the discovery of electron in 1897, he argued that atoms are composed of charged particles and that the light originated from their oscillations in an atom. Later, he proposed the so-called Lorentz oscillator model (LOM) to account for the anomalous dispersion in dielectric substances in the framework of classical physics. Besides, he published research papers on general theory of relativity and delivered lectures on Schrödinger's wave mechanics. Interestingly,

he spent nearly eight years in developing mathematical models for flood control dams in his country, the Netherlands, and his findings have been recognized
as one of the greatest works in hydraulic engineering. In fact, the dictum 'talent hits a target that others miss, and genius hits a target that others do not even see' by the celebrated 19th century German philosopher Schopenhauer appropriately describes spectacular creative work carried out by the legendary Lorentz.

In the end of 1905, when the structure of atoms was not yet established, Lorentz in his paper entitled 'The absorption and emission lines of gaseous bodies', put forward the idea that in the presence of an oscillating electric field, electrons in an atom behave as driven velocity-dependent-damped harmonic oscillators – the LOM [2]. The formulae derived by using the time-dependent position vector of these electrons quite well describe the electric polarization and, hence, dielectric function and optical properties of various types of materials [3-12]. In other words, the LOM provides a classical theory for understanding interaction between electromagnetic (e.m.) radiation and matter. It is indeed amazing that despite being a completely classical concept, in later works, this model fitted adequately in the realm of quantum mechanics and has been fruitfully used in analyzing various electrical and optical properties of insulators, undoped as well as doped semiconductors, and ionic crystals [3,6,9,10,12]. In fact, strictly speaking all these features of solids are properly explained in terms of band structure, which is an outcome of their quantum mechanical description.

Recently, with a view to incorporating some quantum mechanical aspects in the formalism of this model, the oscillator has been quantized using the Bohr and the Bohr-Sommerfeld theories and quantum mechanical selection rules, establishing relationship between the oscillator impedance and the energy eigenvalues of hydrogen-like atoms [13,14]. Model so obtained has been named quantum impedance Lorentz oscillator by the authors - Zhao and coworkers. They have shown that their modified model can be used to analyze linear and nonlinear properties of many dielectric materials containing hydrogen-like atoms.

However, prior to introduction of LOM, Drude (1900, just 3 years after the discovery of electron), in his publication on 'electron theory of metals', assumed that a metal is composed of positively charged immobile particles submerged in a sea of mobile negatively charged electrons. He treated the motion of electron gas as classical entities under the influence of constant uniform electric field in the framework of kinetic theory, with positive particles as scattering centers and obtained an expression for DC conductivity of metals. In fact, the Drude model (DM) can be treated as a special case of LOM and has been found to be very useful in getting insight into the optical properties of metals.

It is interesting to note that despite their numerous shortcomings, a combination of DM and LOM is quite commonly used to analyze experimental data for optical properties of conducting materials. It is usually referred to as Drude-Lorentz Oscillator Model (DLOM). Besides, some improved versions making use of the concepts of these models and even including confining potentials have also been developed. These are applicable not only to bulk materials but also to nanoparticles and systems falling under the purview of nonlinear optics. Of course, these have their own merits and demerits. Some of the relevant references have been well summarized in [15]. It may also be mentioned that some softwares based on the LOM and DLOM are available for analysis of optical spectra of solids.

The principal purpose of this article is to delineate upon LOM and derivation of expressions for different electric and optical quantities, and to discuss the DM for metals (as a special case of LOM). In fact, both these models provide fairly good qualitative results for some solids and are, therefore, quite useful in making preliminary predictions. Some illustrative examples of these models and DLOM have also been included.

2 The Lorentz Oscillator and its Solution

Following Lorentz, we take an atom to be composed of an electron of electric charge $-q$ and mass m bound to an infinitely massive stationary nucleus / positive ion core by a hypothetical spring characterized by force constant k. On being slightly displaced from its equilibrium position, the classically treated electron executes simple harmonic motion of natural or free angular frequency $\omega_0 = \sqrt{k/m}$. Sometimes, the characteristic frequency ω_0 is referred to as fundamental or resonant frequency. This oscillatory motion experiences a velocity-dependent viscous resistance or damping, with coefficient γ, caused by collisions, radiative losses, etc. In the presence of an external harmonic electric field of angular frequency Ω, $\boldsymbol{E}(t) = \boldsymbol{E_0}e^{-i\Omega t}$(as it occurs in the description of travelling e.m. waves), the electron becomes a driven damped harmonic oscillator described by the following equation of motion,

$$\ddot{\boldsymbol{r}}(t) + \gamma\dot{\boldsymbol{r}}(t) + \omega_0^2\boldsymbol{r}(t) = -\frac{q}{m}\boldsymbol{E_0}e^{-i\Omega t}. \quad (1)$$

Here, $\boldsymbol{r}(t)$ is the instantaneous displacement of the electron from its equilibrium position. Note that γ has dimension of inverse time and is, therefore, also called damping rate. It may be pointed out that the Lorentz force arising from the interaction of electronic charge with the magnetic field of an e.m. wave has been omitted because the electron velocity is very small as compared to the speed of light.

As demonstrated in the Appendix, for sufficiently large times the complementary solution of Eq. (1) giving rise to transients will vanish and only the particular integral, is left. Thus, the steady state solution can be written as

$$\boldsymbol{r}(t) = -\frac{q}{m}\frac{1}{(\omega_0^2-\Omega^2)-i\gamma\Omega}\boldsymbol{E_0}e^{-i\Omega t} = -\frac{q}{m}\left\{\frac{(\omega_0^2-\Omega^2)+i\,\gamma\Omega}{(\omega_0^2-\Omega^2)^2+(\gamma\Omega)^2}\right\}\boldsymbol{E_0}e^{-i\Omega t}. \quad (2)$$

We have not used any subscript with $\boldsymbol{r}(t)$ to indicate steady state, for convenience. Note that in this state the electron oscillates with the angular frequency Ω of the field. In fact, explicit dependence of $\boldsymbol{r}(t)$ on Ω is quite clear from Eq. (2). Furthermore, it is implicitly assumed that the motion of the electron is such that it is always associated with the same nucleus / ion core.

Writing $(\omega_0^2 - \Omega^2) = A\cos\theta$ and $\gamma\Omega = \mathrm{A}\sin\theta$ so that $A = \{(\omega_0^2 - \Omega^2)^2 + (\gamma\Omega)^2\}^{1/2}$ and $\theta = tan^{-1}\{\gamma\Omega/(\omega_0^2 - \Omega^2)\}$, Eq. (2) becomes

$$\boldsymbol{r}(t) = -\frac{q}{m}\frac{1}{\left\{(\omega_0^2-\Omega^2)^2+(\gamma\Omega)^2\right\}^{1/2}}\boldsymbol{E_0}e^{-i(\Omega t-\theta)}. \quad (3)$$

It may be noted that the complex nature of the amplitude in Eq. (2) has been taken care of by introducing the phase angle θ. Furthermore, Eq. (3) shows that at any time t, the displacement of the oscillating electron lags behind the driving electric field $\boldsymbol{E}(t)$ by an angle θ. In other words, there is a time delay between the applied field and the resulting motion of the electron. Obviously, the phase difference θ is quite small when $\Omega \ll \omega_0$ $(\Omega \to 0)$, rises to $\pi/2$ for Ω close to ω_0 and further increases to π when $\Omega \gg \omega_0 (\Omega \to \infty)$. Also, for a specific value of γ, the denominator in the expression in Eq. (3) is minimum and the amplitude is maximum when $\Omega = \omega_0$. This justifies ω_0 being called the resonant frequency.

3 Dielectric Materials in the Framework of LOM

Recall that an electric dipole is an arrangement of two equal and opposite charges $(\pm Q)$ separated by a distance r. It has dipole moment $\boldsymbol{p} = Q\boldsymbol{r}$, where $\boldsymbol{r}$ and, hence, $\boldsymbol{p}$ is a vector directed from negative charge to the positive one. When an atom is subjected to an external static uniform electric field, the electron orbits (particularly those of the valence electrons) get distorted and the otherwise coincident centers of positive and negative charges (the nucleus and the electron cloud, respectively) get shifted relative to each other because these experience forces in opposite direction. These so

displaced charges create an electric dipole whose moment is aligned along the field and the atom is said to be polarized. In other words, the applied electric field induces a dipole moment in the atom. If the applied electric field is oscillatory in nature, then the separation between the centres of positive and negative charges will also be oscillatory and this will lead to an electric dipole with oscillatory moment. In the LOM, since the electron is taken as a classical particle it can be assumed to be located at the position of maximum probability of the electron cloud. Furthermore, as the nucleus has been assumed to be infinitely heavy, the applied electric field $\boldsymbol{E}(t)$ causes a shift only in the electron (which now behaves as a forced oscillator). In the present discussion, $\boldsymbol{r}(t)$ has been assumed to be directed from the stationary positive nucleus / ion core to the negatively charged electron, which is opposite to the sign convention for the electric dipole. Accordingly, the instantaneous electric dipole moment induced by the displaced electron in the associated atom (in the framework of LOM) will be given by $-\boldsymbol{p}(t) = q\boldsymbol{r}(t)$**.** Substituting for $\boldsymbol{r}(t)$ from Eq. (2) and using $\boldsymbol{E}(t)$ in place of $\boldsymbol{E_0}e^{-i\Omega t}$ there, we have

$$\boldsymbol{p}(t) = \frac{q^2}{m}\left\{\frac{(\omega_0^2-\Omega^2)+i\,\gamma\Omega}{(\omega_0^2-\Omega^2)^2+(\gamma\Omega)^2}\right\}\boldsymbol{E}(t). \qquad (4)$$

Note that $\boldsymbol{p}(t)$ is also given by $\varepsilon_0\alpha(\Omega)\boldsymbol{E}(t)$, where $\varepsilon_0 = 8.85\times10^{-12}$ F m^{-1} is electric permittivity of vacuum and $\alpha(\Omega)$ is atomic polarizability determined by the exact structure of the atom. Equating these two expressions for $\boldsymbol{p}(t)$, we get Lorentz polarizability for an atom as

$$\alpha(\Omega) = \frac{q^2}{m\varepsilon_0}\left\{\frac{(\omega_0^2-\Omega^2)+i\,\gamma\Omega}{(\omega_0^2-\Omega^2)^2+(\gamma\Omega)^2}\right\}. \qquad (5)$$

Thus, both $\boldsymbol{p}(t)$ and $\alpha(\Omega)$ are complex quantities.

If the number of such electrons per unit volume (in some material) is N , then instantaneous complex electric polarization (which is dipole moment per unit volume) of the collection will be

$$\boldsymbol{P}(t) = N\boldsymbol{p}(t) = \frac{Nq^2}{m}\left\{\frac{(\omega_0^2-\Omega^2)+i\,\gamma\Omega}{(\omega_0^2-\Omega^2)^2+(\gamma\Omega)^2}\right\}\boldsymbol{E}(t). \quad (6)$$

Here, we have assumed that response of all the electrons in the solid is identical so that all of these have the same $\boldsymbol{p}(t)$. Once again, $\boldsymbol{P}(t)$, which is macroscopic property of the substance, also depends upon Ω and is out of phase with respect to $\boldsymbol{E}(t)$ as discussed at the end of section 2. Now, polarization is related to electric susceptibility $\chi(\Omega)$ **,** sometimes referred to as first-order susceptibility, through $\boldsymbol{P}(t) = \varepsilon_0\chi(\Omega)\,\boldsymbol{E}(t)$ so that

$$\chi(\Omega) = N\alpha(\Omega) = \frac{Nq^2}{m\varepsilon_0}\left\{\frac{(\omega_0^2-\Omega^2)+i\,\gamma\Omega}{(\omega_0^2-\Omega^2)^2+(\gamma\Omega)^2}\right\}. \quad (7)$$

While writing the preceding expression for $\boldsymbol{P}(t)$, it is presumed that the material is isotropic in nature. Note that $\sqrt{Nq^2/m\varepsilon_0}$ has dimensions of angular frequency and is called plasma frequency, which is characteristic of the material. Denoting this by ω_p , we have

$$\chi(\Omega) = \omega_p^2\left\{\frac{(\omega_0^2-\Omega^2)+i\,\gamma\Omega}{(\omega_0^2-\Omega^2)^2+(\gamma\Omega)^2}\right\}, \qquad (8)$$

which too is complex.

Next, electric permittivity of a dielectric material is given by $\varepsilon = \varepsilon_0\varepsilon_r$, where $\varepsilon_r\ (= 1+\chi)$ is known as relative electric permittivity of the medium. Thus,

$$\varepsilon_r(\Omega) = 1 + \omega_p^2\left\{\frac{(\omega_0^2-\Omega^2)+i\,\gamma\Omega}{(\omega_0^2-\Omega^2)^2+(\gamma\Omega)^2}\right\}. \qquad (9)$$

Obviously, $\varepsilon_r(\Omega)$ too is a complex quantity and is also referred to as dielectric function. For $\Omega\to0$, the so-called DC limit or static value of the external electric field, Eq. (9) gives $\varepsilon_r(0) \equiv \varepsilon_r(\Omega\to0) = 1+(\frac{\omega_p}{\omega_0})^2$. Similarly, at the other extreme, when $\Omega\to\infty$, we have $\varepsilon_r(\infty) \equiv \varepsilon_r(\Omega\to\infty = 1$. Note that both ε_r0 and $\varepsilon_r\infty$ are real and independent of damping coefficient γ. Combining these two results, we get

$$\omega_p^2 = \omega_0^2\{\varepsilon_r(0) - \varepsilon_r(\infty)\}. \qquad (10)$$

Hence, Eq. (9) can also be written as

$$\varepsilon_r(\Omega) = \varepsilon_r(\infty) + \left[\frac{\omega_0^2\{\varepsilon_r(0)-\varepsilon_r(\infty)\}\{(\omega_0^2-\Omega^2)+i\,\gamma\Omega\}}{(\omega_0^2-\Omega^2)^2+(\gamma\Omega)^2}\right]. \qquad (11)$$

Now, writing $\varepsilon_r(\Omega) = \varepsilon_r'(\Omega) + i\varepsilon_r''(\Omega)$, and thus separating the real and imaginary parts in Eq. (9), we have

$$\varepsilon_r'(\Omega) = 1 + \frac{\omega_p^2(\omega_0^2-\Omega^2)}{(\omega_0^2-\Omega^2)^2+(\gamma\Omega)^2} \qquad (12)$$

and

$$\varepsilon_r''(\Omega) = \frac{\omega_p^2\gamma\Omega}{(\omega_0^2-\Omega^2)^2+(\gamma\Omega)^2}\,. \qquad (13)$$

We can also use Eq. (10) to eliminate ω_p^2 in these expressions. Note that for a particular value of other parameters, both $\varepsilon_r'(\Omega)$ and $\varepsilon_r''(\Omega)$ will decrease with increase in the value of γ. It may also be pointed out that $\varepsilon_r''(\Omega)$ vanishes when either $\Omega = 0$ or $\gamma = 0$. This implies that the imaginary part of dielectric function is intimately associated with oscillatory nature of applied electric field and damping. Thus, it is an outcome of dissipation of energy of the oscillatory external field in the medium.

It may be noted that the sign of the term added to unity in Eq. (12) will be positive or negative depending on whether Ω is smaller or larger than ω_0. Thus, this term is antisymmetric with respect to ω_0. It must be emphasized that $\varepsilon_r'(\Omega)$ will certainly be positive for $\Omega < \omega_0$, while its sign for $\Omega > \omega_0$ will be determined by the relative magnitudes of the second term and unity. On the other hand, Eq. (13) is always positive whether $\Omega < \omega_0$ or $\Omega > \omega_0$ implying that $\varepsilon_r''(\Omega)$ is symmetric about ω_0 and it will never become negative.

As a follow up of the statement made after Eq. (9), we note that $\varepsilon_r'(0) = 1 + (\frac{\omega_p}{\omega_0})^2$, $\varepsilon_r'(\infty) = 1$, and $\varepsilon_r''(0) = \varepsilon_r''(\infty) = 0$. We now look at the physical aspects of the result pertaining to the imaginary part of the dielectric function in the light of the statements made after Eq. (13). In the DC limit, all the dipoles are essentially aligned along the applied electric field (which is basically static), and these do not undergo any movement as there is no change in the field. Therefore, there is no energy loss at all and $\varepsilon_r''(0) = 0$. On the other hand, when the electric field frequency Ω is extremely large, the oscillations of the induced dipoles fail to keep pace with this because their natural frequency is quite small as compared to Ω and again there is no movement. The consequent absence of energy dissipation results in $\varepsilon_r''(\infty) = 0$.

However, if Ω has a nonzero finite value then we consider the following cases.

(i) If interaction of the oscillating electrons with their surroundings is negligible so that damping can be taken as zero for all values of Ω, then substituting $\gamma = 0$ into Eqs. (12) and (13), we get

$$\varepsilon_r'(\Omega) = 1 + \frac{\omega_p^2}{(\omega_0^2-\Omega^2)} \qquad (14)$$

and

$$\varepsilon_r''(\Omega) = 0. \qquad (15)$$

Clearly, $\varepsilon_r'(\Omega)$ will tend to $+\infty$ when Ω approaches ω_0 from below and it will be $-\infty$ for Ω approaching ω_0 from above, with a discontinuity at $\Omega = \omega_0$ (the resonance frequency). Furthermore, $\varepsilon_r''(\Omega) = 0$ implies no energy loss, which is a consequence of γ being zero.

(ii) From Eq. (12), it is clear that $\varepsilon_r'(\Omega)$ will be zero, if $\omega_p^2(\omega_0^2 - \Omega^2) = -\{(\omega_0^2 - \Omega^2)^2 + (\gamma\Omega)^2\}$. Solving this quartic equation in Ω, we find that $\varepsilon_r'(\Omega) = 0$, when $\Omega_0 = \sqrt{\frac{1}{2}\{A \pm \sqrt{B}\}}$, where $A = \omega_p^2 + 2\omega_0^2 - \gamma$ and $B = \omega_p^4 - \gamma^2(2\omega_p^2 + 4\omega_0^2 - \gamma^2)$. Since angular frequency cannot be negative, we have considered only the positive root for Ω_0. Thus, $\varepsilon_r'(\Omega)$ versus Ω plot will cross the Ω −axis twice. However, if

$\gamma > \left\{2\omega_0^2 + \omega_p^2 - 2\omega_0\sqrt{\omega_0^2 + \omega_p^2}\right\}^{1/2}$, then B becomes negative making Ω_0 a complex quantity meaning thereby that $\varepsilon_r'(\Omega)$ never becomes zero and remains positive for all values of Ω. Furthermore, for negligibly small values of γ, $A \approx \omega_p^2 + 2\omega_0^2$ and $B \approx \omega_p^4$ so that $\Omega_0 \approx \omega_0$ and $\sqrt{\omega_0^2 + \omega_p^2}$. In fact, these cross overs of $\varepsilon_r'(\Omega)$ can be used to guess values of ω_0 and ω_p for fitting the experimental data to this model.

(iii) If the applied field frequency Ω is reasonably smaller than ω_0 and γ is also such that $(\gamma\Omega)^2$ can be neglected as compared to $(\omega_0^2 - \Omega 22$, then Eqs. (12) and (13) become $\varepsilon_r'(\Omega \ll \omega_0) \approx 1 + \frac{\omega_p^2}{(\omega_0^2 - \Omega^2)}$ and $\varepsilon_r''(\Omega \ll \omega_0) \approx 0$. To look at, these are the same expressions as obtained in Eqs. (14) and (15) but here $\Omega \ll \omega_0$ (very low applied-field frequency limit). Also, γ and ε_r'' have nonzero but extremely small values.

(iv) For $\Omega = \omega_0$, $\varepsilon_r'(\omega_0) = 1$ and $\varepsilon_r''(\omega_0) = \omega_p^2/\gamma\omega_0$. Thus, the former is unity for all γ, while the latter varies inversely as γ.

(v) When the driving field frequency Ω is significantly larger than ω_0 so that $(\omega_0^2 - \Omega^2) \approx -\Omega^2$ and γ is nonzero but small enough that $(\gamma\Omega)^2 \ll (\omega_0^2 - \Omega^2)^2$, then from Eqs. (12) and (13), we have

$$\varepsilon_r'(\Omega \gg \omega_0) \approx 1 - \left(\frac{\omega_p}{\Omega}\right)^2 \qquad (16)$$

and

$$\varepsilon_r''(\Omega \gg \omega_0) \approx 0. \qquad (17)$$

Thus, for sufficiently large Ω, $\varepsilon_r' < 0$ for $\Omega < \omega_p$ and it becomes positive when $\Omega > \omega_p$.

The preceding considerations reveal that for Ω away from ω_0, $\varepsilon_r''(\Omega)$ is quite small as compared to $\varepsilon_r'(\Omega)$ and it becomes more important when the value of Ω is close to that of ω_0. Thus, the dielectric function will behave as a complex quantity (implying energy losses) mainly for applied field frequencies near the natural frequency.

Next, extrema in ε_r' as function of Ω occur when $\frac{d\varepsilon_r'(\Omega)}{d\Omega} = 0$. Simplifying the expression so obtained, we finally get the relevant physically meaningful values of Ω as $\Omega_1' = \omega_0\sqrt{1 - (\gamma/\omega_0)}$ and $\Omega_2' = \omega_0\sqrt{1 + (\gamma/\omega_0)}$ with the restriction that $\gamma < \omega_0$. Thus, in the presence of damping, $\Omega_1' < \omega_0$ and $\Omega_2' > \omega_0$. The corresponding values of $\varepsilon_r'(\Omega)$ are found to be

$$\varepsilon_r'(\Omega_1') = 1 + \frac{\omega_p^2}{\gamma(2\omega_0 - \gamma)} \qquad (18)$$

and

$$\varepsilon_r'(\Omega_2') = 1 - \frac{\omega_p^2}{\gamma(2\omega_0 + \gamma)}. \qquad (19)$$

Obviously, the former is local maximum (peak) while the latter is local minimum (dip). Also, since $\gamma < \omega_0$, $\varepsilon_r'(\Omega_1')$ will always be positive irrespective of the value of γ. On the other hand, $\varepsilon_r'(\Omega_2')$ will be negative if $\frac{\omega_p^2}{\gamma(2\omega_0 + \gamma)} > 1$, which is so if $\gamma < \omega_0\left(\sqrt{1 + \left(\frac{\omega_p}{\omega_0}\right)^2} - 1\right)$. For higher values of γ, $\varepsilon_r'(\Omega_2')$ will be positive.

To make the above-mentioned aspects visually clear, we have plotted $\varepsilon_r'(\Omega)$ vs Ω for Eq. (12) in Figs. 1 and 2. Note that the parameters ω_0, ω_p, and γ appearing in this equation have units rad s^{-1} and their magnitudes are $\sim 10^{15}$ or so. However, we shall express these in energy units, eV, by multiplying with $\hbar = 6.58 \times 10^{-16}$ eV s^{-1}. Thus, strictly speaking ω_0, ω_p, and γ as used hereafter are $\hbar\omega_0$, $\hbar\omega_p$, and $\hbar\gamma$, respectively. Accordingly, Ω too is taken in eV and refers to photon energy. It may be mentioned that Ω lies between 1.65 and 3.26 eV for the visible region.

Guided by the fact that for a good number of dielectric materials ω_p and ω_0 lie between 10 and 15 eV, and between 8 and 13 eV, respectively, we have taken $\omega_p = 13.5$ eV and $\omega_0 = 10$ eV. In fact, these are the values we have later used for fitting the experimental data for silica in Section 5. Note

that both the chosen values are in the extreme ultraviolet region. The γ values used in Fig. 1 are 0, 0.05 and 0.2 eV while these are 1.0, 4.0 and 7.0 eV for Fig. 2. In Fig.1, the Ω values have been taken from 9 eV to 11 eV and $\varepsilon_r'(\Omega)$ values from -300 to 300 rather than the actual values obtained, to make the plots for non-zero γ to be clearly noticeable. Consequently, the Ω values higher than ω_0 , for which $\varepsilon_r'(\Omega)$ undergoes change from negative values to positive ones are not visible. In all the cases depicted in Fig. 1, $\varepsilon_r'(\Omega)$ changes sign at $\Omega \approx 16.8$ eV, which is

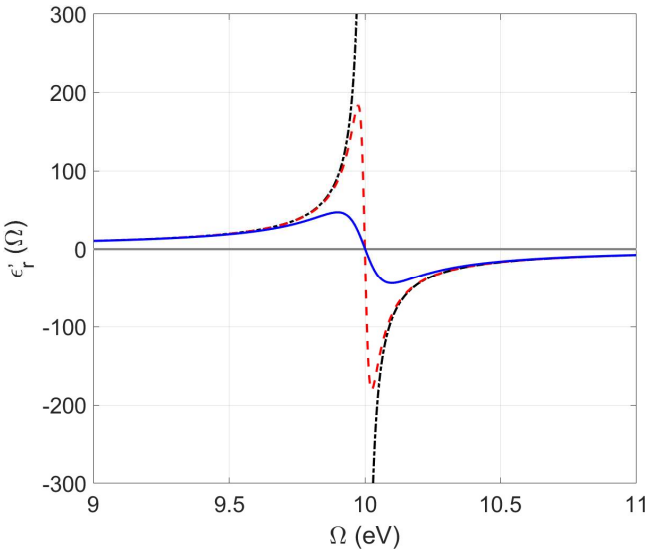

Fig. 1. Plots showing angular frequency dependence of $\varepsilon_r'(\Omega)$ for $\omega_p = 13.5$ eV, $\omega_0 = 10$ eV, and $\gamma = 0$ (black dash-dot line), $\gamma = 0.05$ eV (red dashed line), and $\gamma = 0.2$ eV (blue solid line).

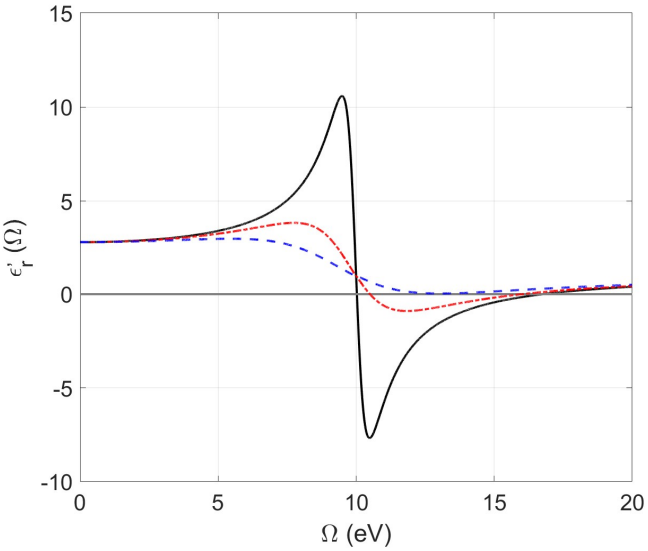

Fig. 2. $\varepsilon_r'(\Omega)$ vs Ω plots for $\omega_p = 13.5\,eV$, $\omega_0 = 10\,eV$, and $\gamma = 1.0$ eV (black solid line), $\gamma = 4.0$ eV (red dash-dot line), and $\gamma = 7.0$ eV (blue dash-dash line).

consistent with the value determined from $\Omega_0 = \sqrt{\omega_0^2 + \omega_p^2}$ found earlier. As far as higher values of γ are concerned, in Fig. 2 the crossover occurs at $\Omega_0 = 16.61$ eV for $\gamma = 1.0$ eV, and at $\Omega_0 = 16.0$ eV for $\gamma = 4.0$ eV. However, sign does not change for $\gamma = 7.0$ eV.

Coming to the expression for $\varepsilon_r''(\Omega)$, Eq. (13), the condition for occurrence of extrema in ε_r'', which is always positive, as function of Ω leads to local maximum (peak) at

$$\Omega'' = \left[\frac{2\omega_0^2 - \gamma^2}{6}\left\{1 + \sqrt{1 + \frac{12\omega_0^4}{(2\omega_0^2 - \gamma^2)^2}}\right\}\right]^{1/2}. \quad (20)$$

For very small value of γ ($\ll \omega_0$), Ω'' is quite close to ω_0 and decreases slightly with increase in γ; in fact, Ω''= 0.97 ω_0 when $\gamma = 0.5\ \omega_0$.

The above consideration shows that the peak in $\varepsilon_r''(\Omega)$ essentially occurs for Ω reasonably near ω_0. Now, for $\Omega \approx \omega_0$, $\omega_0^2 - \Omega^2 = (\omega_0 + \Omega)(\omega_0 - \Omega) \approx 2\omega_0(\omega_0 - \Omega)$. Accordingly, Eq. (13) for $\varepsilon_r''(\Omega)$ can be written as

$$\varepsilon_r''(\Omega \approx \omega_0) \approx \frac{\omega_p^2}{2\omega_0}\left\{\frac{\frac{\gamma}{2}}{(\omega_0-\Omega)^2+\left(\frac{\gamma}{2}\right)^2}\right\}. \qquad (21)$$

Here, the expression in $\{...\}$ is π times the Lorentzian function with peak at $\Omega = \omega_0$ and γ as full width at half maximum. Therefore, $\varepsilon_r''(\Omega)$ vs Ω plot (which is clearly symmetric with respect to ω_0) is usually said to have Lorentzian shape. It is clear from Eq. (21) that the location of the peak in the $\varepsilon_r''(\Omega)$ graph is given by ω_0 and the peak height is determined by $\omega_p^2/\omega_0\gamma$. Since $\varepsilon_r''(\Omega)$ represents dissipation of energy of the oscillatory field, its peak position ω_0 is sometimes called the absorption angular frequency. Also, the range of Ω values for which magnitude of $\varepsilon_r''(\Omega)$ is large is referred to as region of resonant absorption. In contrast, if we substitute the preceding expression for $\omega_0^2 - \Omega^2$ into Eq. (12), we get

$$\varepsilon_r'(\Omega) \approx 1 + \frac{\omega_p^2}{2\omega_0}\frac{(\omega_0-\Omega)}{(\omega_0-\Omega)^2+(\gamma/2)^2}. \qquad (22)$$

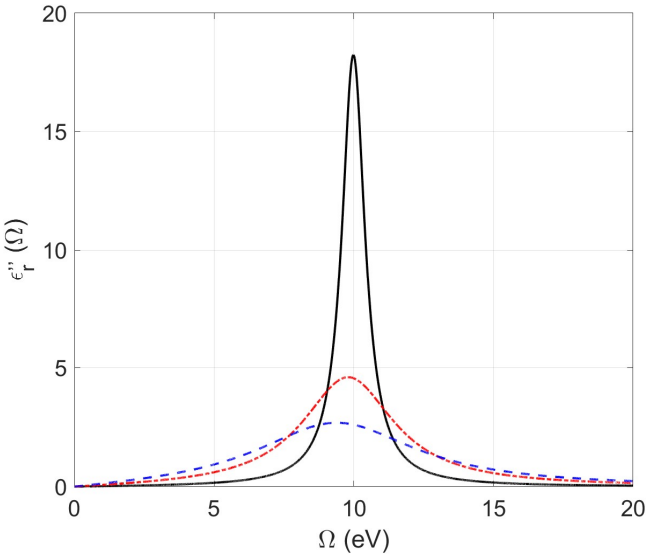

Fig. 3. Variation of $\varepsilon_r''(\Omega)$ with Ω for the parameters and legends as used in Fig. 2.

This too brings out the fact that the second term in this expression is an odd function of $(\omega_0 - \Omega)$ and, hence, antisymmetric about ω_0.

The variation of $\varepsilon_r''(\Omega)$ with the applied field frequency Ω has been projected in Fig. 3, for the parameters used in Fig. 2 and it corroborates the observations made above. It is pertinent to note that the plots are peaked nearly around $\Omega = \omega_0$ with little shift towards lower Ω values as γ increases. Thus, energy absorption is maximum for Ω close to ω_0. Also, from Figs. 1- 3, we note that an increase in damping makes the peaks in $\varepsilon_r'(\Omega)$ and $\varepsilon_r''(\Omega)$ vs Ω plots shorter and broader. This is in consonance with the fact that the value of γ provides a measure of the width of these peaks.

Having dwelt upon various aspects of $\varepsilon_r(\Omega)$, we come to some optical properties of the material. Recall that if the phase velocity of an e.m. wave in a medium is v_{ph}, then its refractive index is given by $n = c/v_{ph} = \sqrt{\varepsilon\mu/\varepsilon_0\mu_0} = \sqrt{\varepsilon_r\mu_r}$, where $\mu\ (= \mu_0\mu_r)$ is magnetic permeability of the substance and μ_r is its relative permeability. For the paramagnetic and diamagnetic substances (the so-called non-magnetic materials), μ_r differs from unity by about $10^{-4} - 10^{-6}$ so that for these, we can take $n(\Omega) = \sqrt{\varepsilon_r(\Omega)}$. Thus, the index of refraction of such a substance is a complex quantity, given by

$$n(\Omega) = \left[1 + \omega_p^2\left\{\frac{(\omega_0^2-\Omega^2)+i\,\gamma\Omega}{(\omega_0^2-\Omega^2)^2+(\gamma\Omega)^2}\right\}\right]^{1/2}. \qquad (23)$$

Writing $n(\Omega) = n'(\Omega) + in''(\Omega)$ and using the fact that $n^2(\Omega) = \varepsilon_r(\Omega) = \varepsilon_r'(\Omega) + i\varepsilon_r''(\Omega)$, we get $\varepsilon_r'(\Omega) = \{n'(\Omega)\}^2 - \{n''(\Omega)\}^2$ and $\varepsilon_r''(\Omega) = 2n'(\Omega)n''(\Omega)$. Eliminating $n''(\Omega)$ from these two equations, and solving the resulting quadratic equation in $\{n'(\Omega)\}^2$, we finally get

$$n'(\Omega) = \left\{\frac{\sqrt{\{\varepsilon_r'(\Omega)\}^2+\{\varepsilon_r''(\Omega)\}^2} + \varepsilon_r'(\Omega)}{2}\right\}^{1/2}. \qquad (24)$$

Similarly, elimination of $n'(\Omega)$ from the preceding two equations yields

$$n''(\Omega) = \left\{\frac{\sqrt{\{\varepsilon_r'(\Omega)\}^2+\{\varepsilon_r''(\Omega)\}^2} - \varepsilon_r'(\Omega)}{2}\right\}^{1/2} . \quad (25)$$

These equations give exact relations for the real and imaginary parts of refractive index in terms of the real and imaginary parts of dielectric function. From Eq. (25), we find that $n''(\Omega)$ is zero or nonzero depending on whether $\varepsilon_r''(\Omega)$ is zero or not. Since $\Omega \neq 0$ for e.m. waves, in view of remarks made in the paragraph after Eq. (13), we infer that imaginary part of the refractive index too has its origin in nonzero value of γ. Hence, it pertains to dissipation or absorption of energy of the e.m. radiation passing through the material. Thus, $n''(\Omega)$ is responsible for the attenuation of the incident beam. The real part $n'(\Omega)$ is the conventional refractive index we come across while discussing transmission of light through a medium. The dependence of refractive index on the frequency of light indicates dispersion.

It may be pointed out that for $\gamma = 0$, $\varepsilon_r'(\Omega)$ and $\varepsilon_r''(\Omega)$ are given by Eqs. (14) and (15), respectively, so that Eqs. (24) and (25) yield

$$n'(\Omega) = \sqrt{\varepsilon_r'(\Omega)} = \left\{1 + \frac{\omega_p^2}{(\omega_0^2-\Omega^2)}\right\}^{1/2}, \quad (26)$$

and $n''(\Omega) = 0$. Thus, e.m. radiation passes through such an ideal medium without any absorption or attenuation.

However, if γ is nonzero but very small and $\Omega \ll$
ω_0, then, since $\varepsilon_r''(\Omega \ll \omega_0) \approx 0$, we get from Eqs. (24) and (25), $n''(\Omega \ll \omega_0) \approx 0$ and $n'(\Omega \ll$ *ω0 ≈εr′Ω≪ω0 =1+ωp2ω02−Ω21/2.* But for $\Omega \ll \omega_0$, $\frac{1}{(\omega_0^2-\Omega^2)} = \frac{1}{\omega_0^2}\left\{1 - \frac{\Omega^2}{\omega_0^2}\right\}^{-1} \approx \frac{1}{\omega_0^2}\left\{1 + \frac{\Omega^2}{\omega_0^2}\right\}$ so that

$$n'(\Omega \ll \omega_0) \approx \left[1 + \frac{\omega_p^2}{\omega_0^2}\left\{1 + \frac{\Omega^2}{\omega_0^2}\right\}\right]^{1/2}. \quad (27)$$

Furthermore, for nonzero but very small γ and $\Omega \gg \omega_0$, which practically is the case for X-ray frequencies, we have on substituting Eqs. (16) and (17) into Eqs. (24) and (25),

$$n'(\Omega \gg \omega_0) \approx \sqrt{\varepsilon_r'(\Omega \gg \omega_0)} = \sqrt{1 - \left(\frac{\omega_p}{\Omega}\right)^2}, \quad (28)$$

and $n''(\Omega \gg \omega_0) \approx 0$. Thus, $n(\Omega \gg \omega_0) \approx n'(\Omega \gg \omega_0)$. Note that, for $\omega_0 \ll \Omega < \omega_p$, $n(\Omega)$ is imaginary implying that in the X-ray region, the dielectric substances having small ω_0 values completely absorb radiation if $\Omega < \omega_p$. However, for $\Omega > \omega_p$, the refractive index is real but less than unity, which corresponds to the situation that phase velocity of the e.m. wave in the material is higher than the speed of light in vacuum. Furthermore, it approaches unity when $\Omega \gg \omega_p$.

The dependence of $n'(\Omega)$ and $n''(\Omega)$ on Ω for the parameters mentioned in the caption for Fig. 2 has been illustrated graphically in Figs. 4 and 5, respectively. A look at these plots shows that $n'(\Omega)$ has peak close to ω_0 and it attains minimum value near $\Omega \approx \omega_p$ and then increases again. The relevant magnitudes depend on γ and the width of the flat part of the minimum decreases as γ increases. On

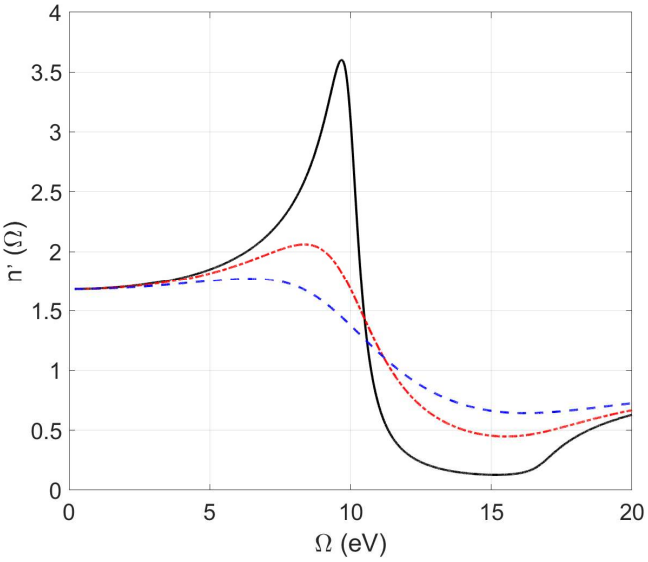

Fig. 4. Spectral dependence of $n'(\Omega)$ for the parameters and legends as described in Fig. 2.

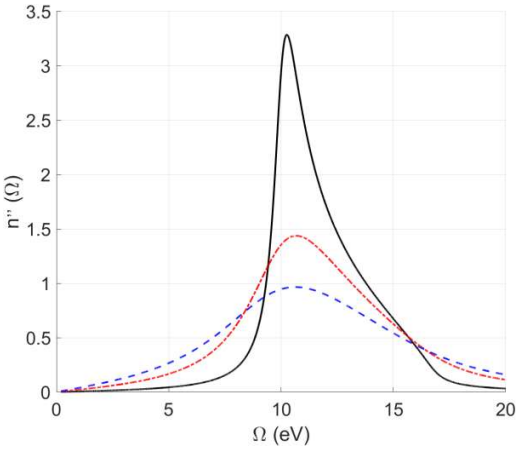

Fig. 5. Dependence of $n''(\Omega)$ on Ω for the parameters and legends as listed in Fig. 2.

the other hand, $n''(\Omega)$ are maximum for Ω lying between ω_0 and ω_p and tend to zero for higher values of Ω. It may be mentioned that the rise in $n'(\Omega)$ values with increase in Ω (i.e., decrease in incident wavelength of e.m. radiation) is known as normal dispersion because this is in accord with what we observe when white light passes through a prism. In contrast the sharp fall in $n'(\Omega)$ with increase in Ω is called anomalous dispersion. It is pertinent to note that anomalous dispersion occurs over the range of Ω values for which $n''(\Omega)$ has its peak (Fig. 5), i.e., the medium is highly absorbing. Consequently, experimental observation of anomalous dispersion is not that easy.

The fact that both $n'(\Omega)$ and $n''(\Omega)$ are quite close to zero for small values of γ and $\Omega \geq \omega_p$ (see Figs. 4 and 5 and Eq. (28)) needs special consideration. As mentioned earlier also, refractive index is obtained by dividing speed of light in vacuum with the phase velocity $v_{ph} = \lambda\,\Omega/2\pi$, where λ is wavelength of the relevant e.m. wave in the medium. Therefore, $n(\Omega) \approx 0$ implies that v_{ph} and, hence, λ are infinitely large. The wavelength being infinite means that all the electrons in the solid are oscillating in phase.

Another physically observable optical quantity of interest is the normal incidence reflection coefficient, reflectivity, or reflectance of the medium. It gives the fraction of the power associated with the incident e.m. wave reflected from the surface of the material. For the air-solid boundary, it is defined as [3,5]

$$R(\Omega) = \left|\frac{n(\Omega)-1}{n(\Omega)+1}\right|^2 = \frac{\{n'(\Omega)-1\}^2+\{n''(\Omega)\}^2}{\{n'(\Omega)+1\}^2+\{n''(\Omega)\}^2}\,. \qquad (29)$$

As a special case, note that for $\Omega \ll \omega_0$ as well as for $\Omega \gg \omega_0$,

$$R(\Omega) \approx \frac{\{n'(\Omega)-1\}^2}{\{n'(\Omega)+1\}^2}\,. \qquad (30)$$

With a view to bring out the dependence of $R(\Omega)$ on various parameters, we have shown $R(\Omega)$ as function of Ω in Fig. 6, for $\omega_p = 13.5$ eV, $\omega_0 = 10$ eV, and $\gamma = 0,\ 0.2,\ 1.0,\ 4.0,$ and 7.0 eV. A perusal of this figure reveals that the damping rounds out the corners of the plots and that an increase in γ decreases the maximum value of reflectance, which is unity or 100% for $\gamma = 0$. Also, for a particular value of γ, $R(\Omega)$ is maximum when

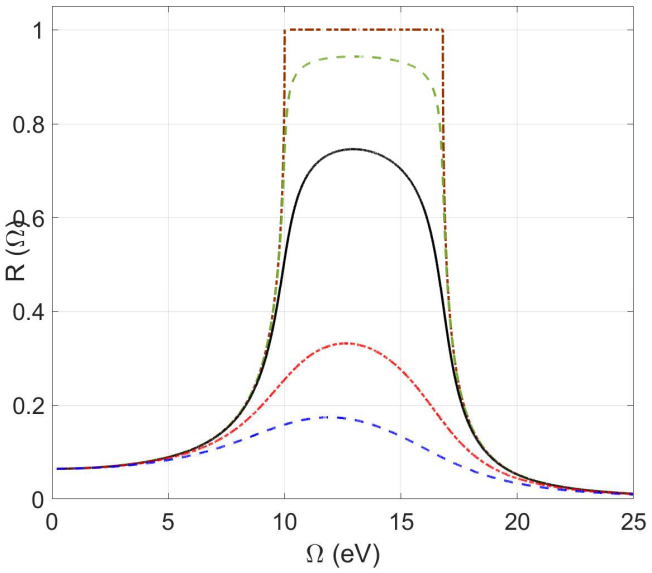

Fig. 6. Reflectivity $R(\Omega)$ vs Ω plots for $\omega_p = 13.5$ eV, $\omega_0 = 10$ eV, and $\gamma = 0.0$ (dark brown

dash-dot line), $\gamma = 0.2$ eV (green dash-dash line) $\gamma = 1.0$ eV (black solid line), $\gamma = 4.0$ eV (red dash-dot line), and $\gamma = 7.0$ eV (blue dash-dash line).

$n'(\Omega)$ is minimum. This is understandable because for $n'(\Omega) \to 0$, Eq. (29) gives $R(\Omega) \to 1$, which is its maximum possible value.

From a perusal of the plots in Figs. 4 – 6 and the discussion of the expressions for $n'(\Omega)$, $n''(\Omega)$, and $R(\Omega)$, it can be inferred that for Ω reasonably smaller than ω_0 and significantly higher than ω_p, the dielectric materials are transparent to the incident e.m. waves. However, for Ω close to ω_0, these show maximum absorption while they are strongly reflective when Ω values lie between ω_0 and ω_p and are even somewhat higher than the latter. In order to make this conclusion clearer, we have shown in Fig. 7, dependence of $n'(\Omega)$, $n''(\Omega)$, and $R(\Omega)$ on Ω for an oscillator system with parameter values $\omega_p = 12$ eV, $\omega_0 = 2.5$ eV, and $\gamma = 1$ eV as a typical representative; here ω_0 is in the visible region and quite less than ω_p, which is at variance with the case depicted in Figs. 4 – 6.

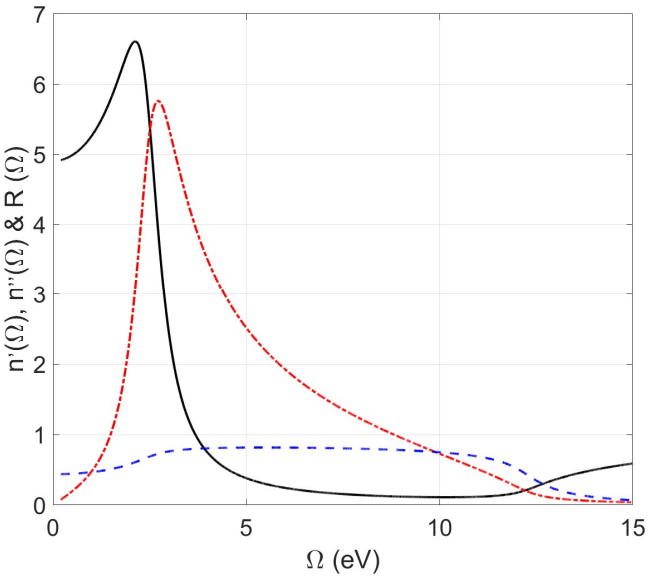

Fig. 7. $n'(\Omega)$ (black solid line), $n''(\Omega)$ (red dash-dot line), and $R(\Omega)$ (blue dash-dash line), as functions of Ω for an oscillator with parameter values $\omega_p = 12$ eV, $\omega_0 = 2.5$ eV, and $\gamma = 1$ eV.

So far, we have assumed that all the Lorentz oscillators in a collection are completely identical. However, a substance can have Lorentz oscillators of different types because the electrons experience different binding and damping forces or the atoms / ion cores with which the electrons are associated have different nature. Suppose that N_j of these in unit volume are of one type represented by subscript j. Denoting their natural angular frequency, and damping coefficient by $\omega_{0,j}$ and γ_j, respectively, the electric susceptibility of this group of Lorentz oscillators will be given by

$$\chi_j(\Omega) = \frac{N_j q^2}{m\varepsilon_0}\left\{\frac{\left(\omega_{0,j}^2-\Omega^2\right)+i\,\gamma_j\Omega}{\left(\omega_{0,j}^2-\Omega^2\right)^2+\left(\gamma_j\Omega\right)^2}\right\}; \quad (31)$$

(see, Eq. (7)). Representing the plasma frequency of this category by $\omega_{p,j}$, we have $\omega_{p,j}^2 = N_j q^2/m\varepsilon_0$ so that

$$\chi_j(\Omega) = \omega_{p,j}^2\left\{\frac{\left(\omega_{0,j}^2-\Omega^2\right)+i\,\gamma_j\Omega}{\left(\omega_{0,j}^2-\Omega^2\right)^2+\left(\gamma_j\Omega\right)^2}\right\}. \quad (32)$$

Also, total electric susceptibility of the system comprising different types of oscillators such that $N = \sum_j N_j$ will be given by $\chi(\Omega) = \sum_j \chi_j(\Omega)$.

Taking the fraction of Lorentz oscillators of type j to be $f_j = N_j/N$, we have $\omega_{p,j}^2 = f_j\omega_p^2$. Accordingly, the relative electric permittivity of this system will be given by

$$\begin{aligned}\varepsilon_r(\Omega) &= 1 + \textstyle\sum_j \chi_j(\Omega)\\ &= 1 + \omega_p^2 \textstyle\sum_j f_j\left\{\frac{\left(\omega_{0,j}^2-\Omega^2\right)+i\,\gamma_j\Omega}{\left(\omega_{0,j}^2-\Omega^2\right)^2+\left(\gamma_j\Omega\right)^2}\right\} \quad (33)\end{aligned}$$

It may be mentioned that f_j is usually referred to as oscillator strength. Also, a quantum mechanical treatment of the problem leads to an expression which looks like Eq. (33) but has different

meaning of $\omega_{0,j}$ as well as f_j . The real and imaginary parts of Eq. (33) are

$$\varepsilon_r'(\Omega) = 1 + \omega_p^2 \sum_j \frac{f_j\left(\omega_{0,j}^2 - \Omega^2\right)}{\left(\omega_{0,j}^2 - \Omega^2\right)^2 + \left(\gamma_j \Omega\right)^2} \qquad (34)$$

and

$$\varepsilon_r''(\Omega) = \omega_p^2 \sum_j \left\{ \frac{f_j \gamma_j \Omega}{\left(\omega_{0,j}^2 - \Omega^2\right)^2 + \left(\gamma_j \Omega\right)^2} \right\}, \qquad (35)$$

respectively. These have been depicted in Fig. 8 for a system comprising two types of oscillators with $\omega_p = 13.5$ eV , $\omega_{0,1} = 10$ eV, $\omega_{0,2} = 12$ eV, $\gamma_1 = \gamma_2 = 1.0$ eV, and $f_1 = f_2 = 0.50$.

While using Eq. (34) for real systems, sometimes the factor 1 on the right-hand side has to be replaced by a greater number corresponding to the value of $\varepsilon_r'(\infty)$ to take care of the contribution of oscillators with higher $\omega_{0,j}$ which are not covered in the summation.

The expression for complex index of refraction is now modified to read

$$n(\Omega) = \left[1 + \omega_p^2 \sum_j f_j \left\{ \frac{\left(\omega_{0,j}^2 - \Omega^2\right) + i\,\gamma_j \Omega}{\left(\omega_{0,j}^2 - \Omega^2\right)^2 + \left(\gamma_j \Omega\right)^2} \right\} \right]^{1/2} \qquad (36)$$

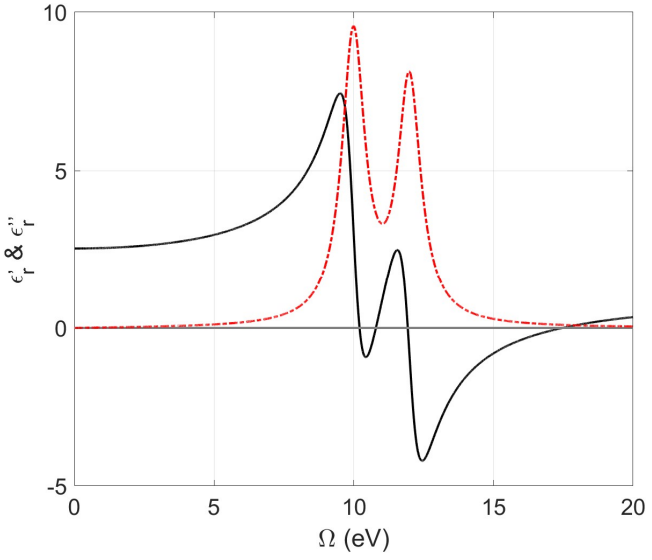

Fig. 8. Spectral dependence of $\varepsilon_r'(\Omega)$ (black solid line) and $\varepsilon_r''(\Omega)$ (red dash-dot line) for a two-oscillator system with $\omega_p = 13.5$ eV, $\omega_{0,1} = 10$ eV, $\omega_{0,2} = 12$ eV, $\gamma_1 = \gamma_2 = 1.0$ eV, and $f_1 = f_2 = 0.5$.

Similarly, Eqs. (24), (25), and (29) for $n'(\Omega)$, $n''(\Omega)$, and $R(\Omega)$, respectively, too are recast for a many-oscillator system. Fig. 9 depicts dependence of these three quantities on Ω for the two-oscillator system considered in Fig. 8.

4 Drude Model for Conducting Substances as an Extension of LOM

According to the DM for a metal the positively charged ion cores are fixed like those in the LOM, but the negatively charged electrons wander around like gas molecules without any constraint of being attached to a particular nucleus or ion core. As such, there is no restoring force acting on an electron and, thus, $\omega_0 = 0$. Furthermore, since an electron is not
hooked up to a specific core, we preferably describe its motion in terms of its instantaneous velocity $\boldsymbol{v}(t)$. However, an electron in the conducting material does experience damping mainly due to its scattering caused by the interaction with the stationary cores, impurities, and crystal imperfections present and with other electrons.

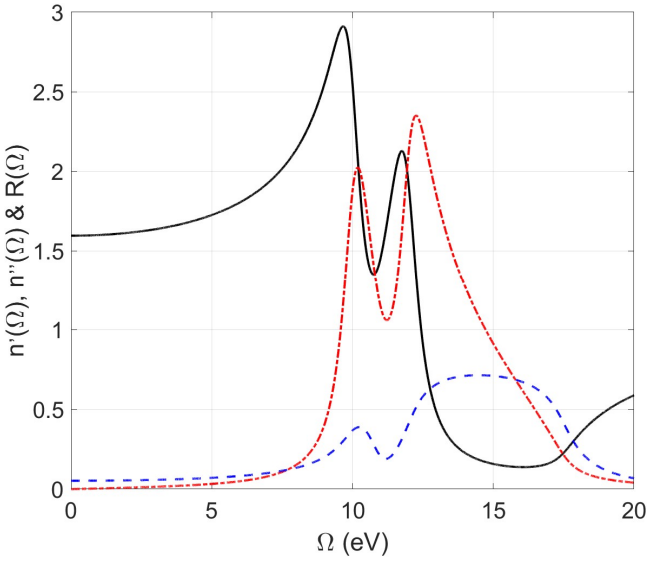

Fig. 9. Plots displaying $n'(\Omega)$ (black solid line), $n''(\Omega)$ (red dash-dot line), and $R(\Omega)$ (blue dash-dash line), as function of Ω for the two-oscillator system having parameter values mentioned in the caption of Fig. 8.

Therefore, the differential equation governing the motion of such an electron under the influence of an applied harmonic electric field $\boldsymbol{E}(t) = \boldsymbol{E_0}e^{-i\Omega t}$, can be written as

$$\dot{\boldsymbol{v}}(t) + \gamma \boldsymbol{v}(t) = -\frac{q}{m}\boldsymbol{E_0}e^{-i\Omega t}. \qquad (37)$$

The homogeneous solution of this first-order nonhomogeneous linear differential equation contains $e^{-\gamma t}$, which becomes zero for large values of t. As in the case of LOM, this too represents transients. Finally, in this case also we are left with the nonhomogeneous solution, the so-called steady state solution, which reads

$$\boldsymbol{v}(t) = -\frac{q}{m}\frac{1}{\gamma - i\Omega}\boldsymbol{E_0}e^{-i\Omega t} = -\frac{q}{m}\frac{\gamma + i\Omega}{\gamma^2+\Omega^2}\boldsymbol{E_0}e^{-i\Omega t}. \qquad (38)$$

Proceeding as has been done in going from Eq. (2) to Eq. (3), it can be shown that $\boldsymbol{v}(t)$, which also oscillates with angular frequency Ω, is out of phase with respect to the external electric field $\boldsymbol{E}(t)$ by an angle $\varphi = tan^{-1}(\Omega/\gamma)$. Obviously, φ increases from 0 to $\pi/2$ as Ω is varied from 0 to extremely large value. In fact, for DC electric field $\boldsymbol{E_0}$ ($\Omega = 0$), velocity is constant and from Eq. (38), it can be written as $\mathbf{v}(\Omega = 0) = -\frac{q\boldsymbol{E_0}}{m\gamma}$. This is called the drift velocity of electrons.

The electric current density produced by all the free electrons with number density N is given by

$$\boldsymbol{J}(t) = -Nq\mathbf{v}(t) = \frac{Nq^2}{m}\frac{\gamma + i\Omega}{\gamma^2+\Omega^2}\mathbf{E}(t). \qquad (39)$$

Since the current density is also given by $\boldsymbol{J}(t) = \sigma(\Omega)\mathbf{E}(t)$, where $\sigma(\Omega)$ is dynamic electrical conductivity of the material, we have

$$\sigma(\Omega) = \frac{Nq^2}{m}\frac{\gamma + i\Omega}{\gamma^2+\Omega^2} = \varepsilon_0\omega_p^2\frac{\gamma + i\Omega}{\gamma^2+\Omega^2}. \qquad (40)$$

This is usually called Drude conductivity and is, obviously, frequency-dependent complex quantity. Here too the solid is taken to be isotropic.

If the applied electric field is constant $\boldsymbol{E_0}$ ($\Omega = 0$), then steady or DC electric current density and corresponding electric conductivity are, respectively, given by $\boldsymbol{J}(\Omega = 0) = \frac{Nq^2}{m\gamma}\boldsymbol{E_0}$ and $\sigma(\Omega = 0) = \frac{Nq^2}{m\gamma}$. Note that this is nothing but Ohm's law with resistivity $\rho = m\gamma/Nq^2$. It may also be pointed out that in this model, all the free electrons contribute to $\boldsymbol{J}$. However, this is in violation of their quantum description, according to which under the influence of applied electric field only a small fraction of electrons in the occupied states below the Fermi level acquire sufficient energy to get excited to the empty energy levels above this to participate in electrical conduction.

Furthermore, the dielectric function $\varepsilon_r(\Omega)$ is related to electrical conductivity $\sigma(\Omega)$ through $\varepsilon_r = 1 + i\frac{\sigma(\Omega)}{\varepsilon_0\Omega}$ so that the Drude complex dielectric function for a conducting material is given by

$$\varepsilon_{r,D}(\Omega) = 1 - \frac{\omega_p^2}{\Omega}\left(\frac{\Omega - i\gamma}{\Omega^2+\gamma^2}\right). \qquad (41)$$

This is the same result as we obtain by putting $\omega_0 = 0$ in Eq. (9) for $\varepsilon_r(\Omega)$ in LOM implying that the DM can be considered as a special case of the Lorentz model. The real and imaginary parts of $\varepsilon_{r,D}(\Omega)$ are

$$\varepsilon'_{r,D}(\Omega) = 1 - \frac{\omega_p^2}{\Omega^2+\gamma^2} \text{ and } \varepsilon''_{r,D}(\Omega) = \frac{\gamma}{\Omega}\frac{\omega_p^2}{\Omega^2+\gamma^2}, \qquad (42)$$

respectively. Note that like $\varepsilon''_r(\Omega)$, $\varepsilon''_{r,D}(\Omega) = 0$ when $\gamma = 0$, meaning thereby that $\varepsilon''_{r,D}(\Omega)$ too is related to damping and, hence, to absorption of energy associated with the applied electric field.

Next, the refractive index of a conducting nonmagnetic material will be given by

$$n_D(\Omega) = \sqrt{\varepsilon_{r,D}(\Omega)} = \left\{1 - \frac{\omega_p^2}{\Omega}\left(\frac{\Omega - i\gamma}{\Omega^2+\gamma^2}\right)\right\}^{\frac{1}{2}}, \quad (43)$$

with relevant expression for the real and imaginary parts $n'_D(\Omega)$ and $n''_D(\Omega)$. Also, Eqs. (24), (25), and (29) too hold good for $n'_D(\Omega)$, $n''_D(\Omega)$, and normal incidence reflectance $R_D(\Omega)$ with appropriate replacement of $\varepsilon'_r(\Omega)$, $\varepsilon''_r(\Omega)$, $n'(\Omega)$, and $n''(\Omega)$.

It may be mentioned that in the case of conducting materials, generally, γ is quite small as compared to ω_p. Now, we consider the following five situations.

(i) For the ideal case $\gamma = 0$, Eqs. (42) and (43) yield

$$\varepsilon'_{r,D}(\Omega) = 1 - \left(\frac{\omega_p}{\Omega}\right)^2, \ \varepsilon''_{r,D}(\Omega) = 0; \quad (44)$$

$$n'_D(\Omega) = \left\{1 - \left(\frac{\omega_p}{\Omega}\right)^2\right\}^{\frac{1}{2}}, \text{ and } n''_D(\Omega) = 0. \quad (45)$$

As expected, the expressions for $\varepsilon'_{r,D}(\Omega)$ and $n'_D(\Omega)$ are special cases of relevant expression in Eqs. (14) and (26) with $\omega_0 = 0$. Note that $\varepsilon'_{r,D}(\Omega)$ is negative for $\Omega < \omega_p$ having quite large magnitude for low values of Ω. It becomes zero when $\Omega = \omega_p$ and increases with increase in Ω value, becoming unity when $\Omega \gg \omega_p$. Furthermore, $n'_D(\Omega)$ and, hence, $n_D(\Omega)$ is imaginary when $\Omega < \omega_p$ implying that the ideal metal is completely opaque to the relevant e.m. radiation. It is less than unity for $\Omega > \omega_p$, and for Ω much larger than ω_p, we can write $n'_D \approx 1 - \frac{1}{2}\left(\frac{\omega_p}{\Omega}\right)^2$.

(ii) For nonzero γ, $\varepsilon''_{r,D}(\Omega)$ is always positive, but $\varepsilon'_{r,D}(\Omega)$ will be negative if $\Omega < \sqrt{\omega_p^2 - \gamma^2}$ and positive for $\Omega > \sqrt{\omega_p^2 - \gamma^2}$. Combined with Eqs. (22) and (23) these imply that $n''_D(\Omega) > n'_D(\Omega)$ for $\Omega < \sqrt{\omega_p^2 - \gamma^2}$ and reverse will be true when $\Omega > \sqrt{\omega_p^2 - \gamma^2}$.

(iii) When Ω is quite small as compared to ω_p and comparable with γ so that $\omega_p^2 \gg \Omega^2 + \gamma^2$, then from Eq. (42) we see that $\varepsilon'_{r,D}(\Omega \ll \omega_p)$ will be negative with quite large magnitude while $\varepsilon''_{r,D}(\Omega \ll \omega_p)$ will be positive and reasonably large depending on the value of γ/Ω. Consequently, $n''_D(\Omega \ll \omega_p)$ will be much larger than $n'_D(\Omega \ll \omega_p)$. Furthermore, dominance of $n''_D(\Omega)$ in the expression for $R(\Omega)$ (Eq. (29)), indicates that $R_D(\Omega \ll \omega_p)$ will be reasonably close to unity. Physically, these features imply that at quite low frequencies ($\Omega \ll \omega_p$), the electric field cannot penetrate the metal and that most of the e.m. radiation will be reflected by it.

(iv) If $\Omega = \omega_p$ implying that $\frac{\omega_p^2}{\gamma^2+\Omega^2} \approx 1$ (assuming that γ is quite small) then $\varepsilon'_{r,D}(\omega_p) \approx 0$ and $\varepsilon''_{r,D}(\omega_p) = \frac{\gamma}{\omega_p} \ll 1$. Thus, both $\varepsilon_{r,D}(\omega_p)$ and $n_D(\omega_p) \approx 0$. However, if γ is not very small then $\varepsilon'_{r,D}(\omega_p)$, $\varepsilon''_{r,D}(\omega_p)$, $n'_D(\omega_p)$ and $n''_D(\omega_p)$ are nonzero and their magnitudes will depend on the value of γ. Furthermore, since $n'_D(\omega_p)$ and $n''_D(\omega_p)$ are nonzero though reasonably small $R_D(\omega_p)$ will still be high and will depend upon the value of γ.

(v) For $\Omega > \omega_p$, $\gamma \ll \Omega$ and $\Omega^2 + \gamma^2 \approx \Omega^2$. Therefore, $\varepsilon'_{r,D}(\Omega > \omega_p) = 1 - \left(\frac{\omega_p}{\Omega}\right)^2 > 0$ and $\varepsilon''_{r,D}(\Omega > \omega_p) \approx 0$. In this case, from Eqs. (24) and (25), we have

$$n'_D(\Omega > \omega_p) \approx \sqrt{\varepsilon'_{r,D}(\Omega > \omega_p)} = \left\{1 - \left(\frac{\omega_p}{\Omega}\right)^2\right\}^{1/2}$$

and $n''_D \approx 0$ so that $R_D(\Omega > \omega_p) \approx \{n'_D(\Omega) - 1\}^2/\{n'_D(\Omega) + 1\}^2$. Thus, $n'_D(\Omega)$ and,

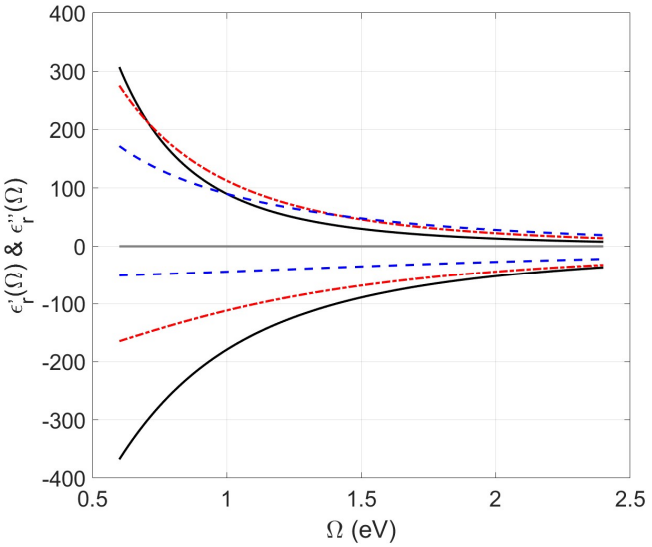

Fig. 10. Plots for $\varepsilon'_{r,D}(\Omega)$ (below the zero line) and $\varepsilon''_{r,D}(\Omega)$ (above the zero line) as function of Ω for a conducting material with $\omega_p = 15$ eV and $\gamma = 0.5$ eV (black solid line), $\gamma = 1.0$ eV (red dash-dot line), and $\gamma = 2.0$ eV (blue dash-dash line). Note that both the axes have been highly truncated.

hence, $n_D(\Omega)$ become nonzero when Ω exceeds ω_p, and attain maximum value 1 for $\Omega \gg \omega_p$. Obviously, $R_D(\Omega \gg \omega_p)$ will be zero. In other words, at very high frequencies, the free electron contribution is unimportant.

To bring out various aspects discussed above, we have plotted $\varepsilon'_{r,D}(\Omega)$ and $\varepsilon''_{r,D}(\Omega)$ as function of Ω for a metal characterized by $\omega_p = 15\ eV$ and $\gamma = 0.5, 1.0,$ and $2.0\ eV$ in Fig. 10. Note that ω_p lies between 9 and 20 eV for most of the conducting materials and that we have taken $\omega_p = 15\ eV$ to analyze the experimental data for aluminium in Section 5. Since magnitudes of $\varepsilon'_{r,D}(\Omega)$ and $\varepsilon''_{r,D}(\Omega)$ are quite high and we wanted to clearly bring out the effect of change in γ value, we have taken Ω values from 0.6 eV to 2.4 eV rather than keeping these sufficiently higher than the ω_p value. However, it must be mentioned that the value of $\varepsilon'_{r,D}(\Omega)$ changes from negative to positive at Ω = 14.99, 14.97, and 14.87 eV for $\gamma = 0.5, 1.0,$ and 2.0 eV, respectively, which are in accord with the relation

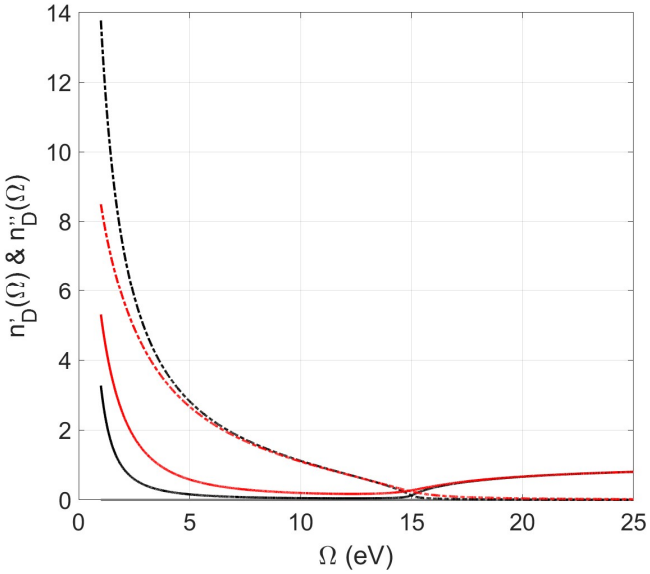

Fig. 11. Graphic representation of $n'_D(\Omega)$ (solid line) and $n''_D(\Omega)$ (dash-dot line) vs Ω for $\omega_p = 15$ eV and $\gamma = 0.5$ eV (black) and 2.0 eV (red).

$\Omega = \sqrt{\omega_p^2 - \gamma^2}$ found above. Furthermore, $\varepsilon'_{r,D}(\omega_p)$ and $\varepsilon''_{r,D}(\omega_p)$ have values 0.001 and 0.033 for $\gamma = 0.5$ eV, and 0.018 and 0.131, respectively, for $\gamma = 2.0$ eV. The corresponding values for $\gamma = 0.1$ eV are 4×10^{-5} and 0.007.

The plots for $n'_D(\Omega)$ and $n''_D(\Omega)$ vs Ω (varied from 1 eV to 25 eV) for $\omega_p = 15$ eV and $\gamma = 0.5$ and 2.0 eV have been projected in Fig. 11. These exhibit predominance of $n''_D(\Omega)$ for $\Omega < \omega_p$. However, for $\Omega > \omega_p, n''_D(\Omega) \approx 0$ and $n'_D(\Omega)$ becomes nonzero approaching 1 for $\Omega \gg \omega_p$. As mentioned in the discussion of case (iv) above, $n'_D(\omega_p)$ as well as $n''_D(\omega_p)$ are nonzero for the γ values considered here. These have values 0.131 and 0.127 for γ = 0.5 eV, and 0.27 and 0.24 for γ = 2.0 eV. However, their values for γ = 0.1 eV are 0.058 and 0.057, respectively.

The effect of γ on the variation of $R_D(\Omega)$ with Ω has been shown by plotting the graphs for $\omega_p = 15$ eV, and $\gamma = 0.0, 0.1, 0.5, 1.0,$ and 2.0 eV in Fig. 12. Here too, the presence of damping leads to

smoothing of corner and departure of the maximum reflectivity from unity. These considerations show

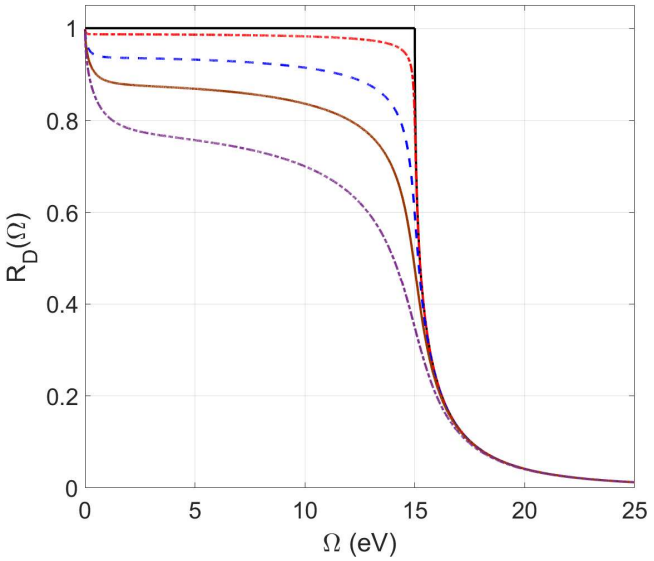

Fig. 12. Spectral dependence of $R_D(\Omega)$ for $\omega_p = 15$ eV, and $\gamma = 0.0$ (black solid line), $\gamma = 0.1$ eV (red dash-dot line), $\gamma = 0.50$ eV (blue dash-dash line), $\gamma = 1.0$ eV (brown solid line), and $\gamma = 2.0$ eV (purple dash-dot line).

that the metals are immensely reflective for the e.m. radiation with frequencies less than their respective plasma frequencies and are transparent when $\Omega > \omega_p$. This explains why metals are very good reflectors of visible light and transparent to x-rays; their ω_p values lie in the ultraviolet region. This situation is sometimes called ultraviolet transparency of metals.

It is worth mentioning that the electrons bound to the atoms in the conducting materials act as Lorentz oscillators and, therefore, analysis of their experimental data pertaining to the electrical and optical properties discussed here must be carried out employing models involving many Lorentz oscillators along with the DM. This arrangement constitutes the so-called DLOM. Furthermore, if the material contains more than one metal then expressions for different physical quantities in the DM are also modified to include more terms with appropriate values of the plasma frequencies, damping constants, and fraction of the electrons of a particular type (see, e.g. [10]).

It is pertinent to point out that the way we have introduced the many oscillators LOM in the preceding section, ω_p is fixed and $\sum_j f_j = 1$. However, while analyzing the optical spectra of materials using this model or its combination with the Drude model (the DLOM), more than one values of ω_p are used and even f_j larger than unity are employed (see, e.g. [9] and [10]).

5 Some Illustrative Applications of LOM, DM and DLOM

In this section, we demonstrate some representative applications of the formulae derived in sections 3 and 4 by considering analysis of experimental data pertaining to optical constants for a wide range of angular frequencies / photon energies in respect of materials of different types. We have directed our attention to optical properties rather than the dielectric functions because the former are themselves defined in terms of the latter and because their experimental investigation is relatively easy. Furthermore, the choice of the examples discussed has mainly been guided by the availability of easily accessible data in the literature.

Before proceeding further, it may, however, be emphasized that our aim is to illustrate the applications and not to claim the high quality of agreement between the model calculations and the experimental data. Otherwise also, as pointed out earlier too, the models discussed in this article are classical in nature and are being used for analyzing the properties which are properly understood in the framework of quantum mechanical description.

(i). Rutile (TiO_2) crystal, which is a large band-gap semiconductor, is a substance having quite a high refractive index in the visible region. It is used for the manufacture of certain optical elements, and in photocatalysis and dilute magnetism. The experimental values of $n'(\Omega)$ and $n''(\Omega)$ for Ω values from 0.83 eV to 6.20 eV have been taken

from [16] and have been used to determine corresponding $R(\Omega)$ values employing Eq. (29). All these optical parameters as function of Ω are shown in Fig. 13. It may be mentioned that $n'(\Omega)$, $n''(\Omega)$,

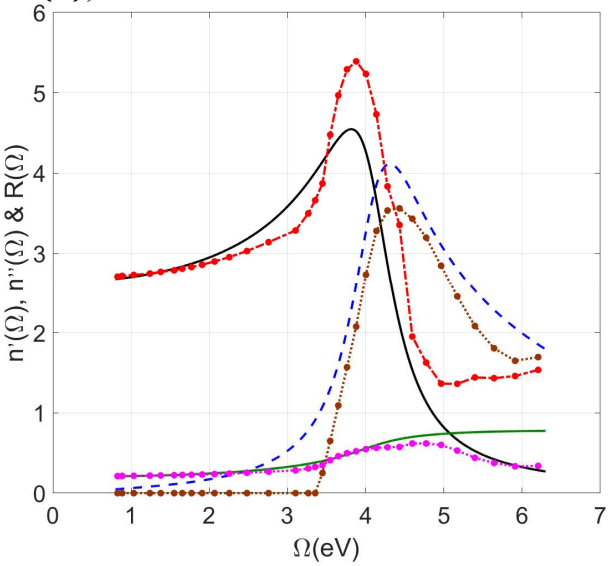

Fig. 13. A comparison of single oscillator-based LOM plots for $n'(\Omega)$ (black solid line), $n''(\Omega)$ (blue dash-dash line), and $R(\Omega)$ (dark green solid line) obtained by using $\omega_p = 10.0\,eV$, $\omega_0 = 4.1\,eV$, and $\gamma = 0.85$ eV with the experimental data [16] for $n'(\Omega)$ (red points and dash-dot line), $n''(\Omega)$ (dark brown points and dot-dot line), and $R(\Omega)$ (pink points and dot-dot line) for TiO_2 crystal.

and $R(\Omega)$ have peaks of 5.39, 3.56, and 0.62 at Ω = 3.88, 4.32, and 4.77 eV, respectively. A reasonably acceptable fit to this single-peak data using the LOM has been obtained with $\omega_p = 10.0\,eV$, $\omega_0 = 4.1\,eV$, and $\gamma = 0.85$ eV. The corresponding plots have also been included in Fig. 13. However, it may be mentioned that model calculations based on $\omega_p = 10.0\,eV$, $\omega_0 = 4.08\,eV$, and $\gamma = 0.60$ eV led to a very good fit for $n'(\Omega)$ but a poor one for $n''(\Omega)$. Similarly, a commendably good fit for $n''(\Omega)$ but not for $n'(\Omega)$ was obtained with $\omega_p = 9.40\,eV$, $\omega_0 = 4.18\,eV$, and $\gamma = 0.95$ eV. However, in both these cases the agreement between model calculations and experimental results for $R(\Omega)$ was relatively poor. In fact, these observations show that a single-oscillator model is inadequate to analyze the data for TiO_2 crystal.

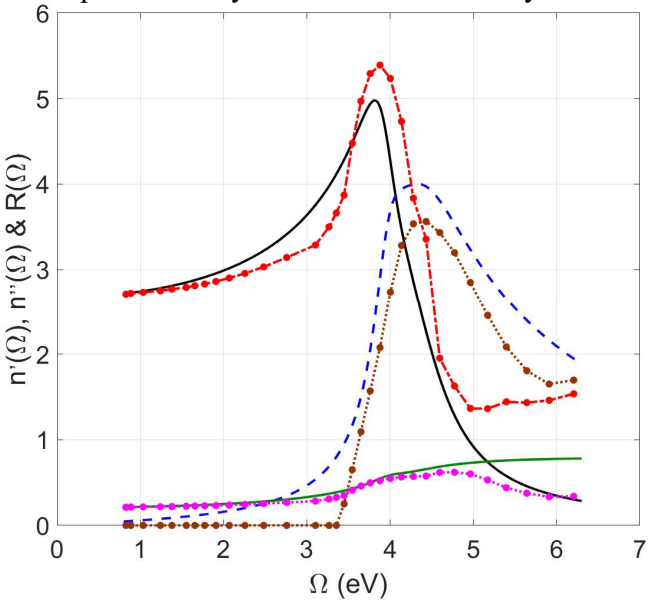

Fig. 14. Model calculations for TiO_2 crystal employing two oscillators with parameters $\omega_p = 10.30\,eV$, ω_{01} = 3.95 eV, $\gamma_1 = 0.45$ eV, f_1= 0. 30, and ω_{02}= 4.25 eV, $\gamma_2 = 1.0$ eV, f_2= 0.70. Legends for the model calculations and the experimental data are the same as in Fig. 13.

Accordingly, a two-oscillator fit was carried out and the outcome together with the parameters used is depicted in Fig. 14. Obviously, the fits are better than those displayed in Fig. 13.

(ii). Silica (SiO_2) is a well-known insulator and is used in microelectronics, in structural materials, in production of glass and optical fibers, and as an additive in the food and pharmaceutical industries. We could get experimental data for SiO_2 crystal for $n'(\Omega)$ up to Ω = 5.91 eV [16] and extracted the values for $n''(\Omega)$ for Ω up to 19.4 eV from Fig.1 in

[15]. These are projected in Fig. 15. Note that the values of $n''(\Omega)$ are close to 0 for Ω up to 8 eV and it has four peaks of magnitudes: 1.48, 1.08, 0.95, and 0.92 at $\Omega = 10.2$, 11.4, 14.2, and 17.2 eV, respectively. We have not calculated experimental $R(\Omega)$ values because of the lack of nonzero values

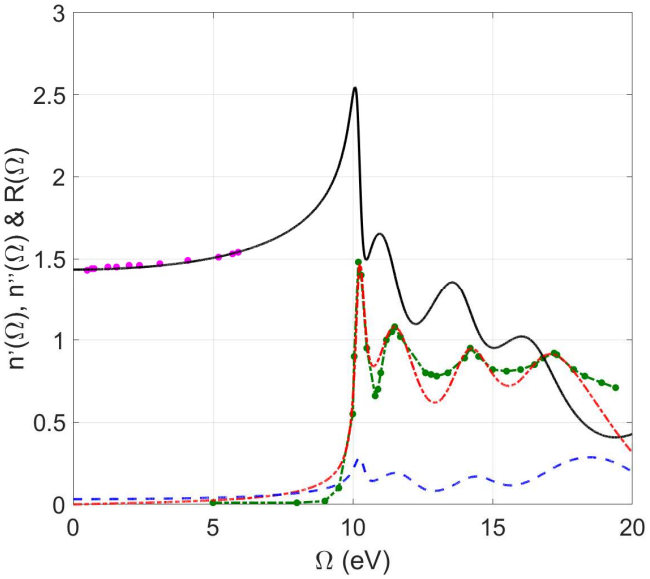

Fig. 15. Plots showing LOM fitting of available experimental data pertaining to $n'(\Omega)$ (pink points [16]) and $n''(\Omega)$ (green points with dash-dot line extracted from Fig. 1 in [15]) for crystalline SiO_2 with four oscillators having parameters $\omega_p = 13.5\,eV$, $\omega_{01} = 10.2$ eV, $\gamma_1 = 0.35$ eV, $f_1 = 0.10$, $\omega_{02} = 11.3$ eV, $\gamma_2 = 1.65$ eV, $f_2 = 0.28$, $\omega_{03} = 14.0$ eV, $\gamma_3 = 1.9$ eV, $f_3 = 0.26$, $\omega_{04} = 16.7$ eV, $\gamma_4 = 2.8$ eV, and $f_4 = 0.36$. The model-based curves are black solid line for $n'(\Omega)$), red dash-dot line for $n''(\Omega)$, and blue dash-dash line for $R(\Omega)$.

of both $n'(\Omega)$ and $n''(\Omega)$ over the same spectral range. A reasonably good fit to the data shown in Fig. 15 has been obtained using four oscillators with parameters listed in the caption to this figure. The model-based plots for $n'(\Omega)$, $n''(\Omega)$, and $R(\Omega)$ are also included in the figure. It should be possible to improve the fit by considering a higher number of oscillators.

(iii). Plots for optical parameters of alkali metals as function of Ω are quite simple and do not show any structure. These are well accounted for by DM. As typical representative of these we have displayed experimental data for reflectivity $R_e(\Omega)$ vs Ω

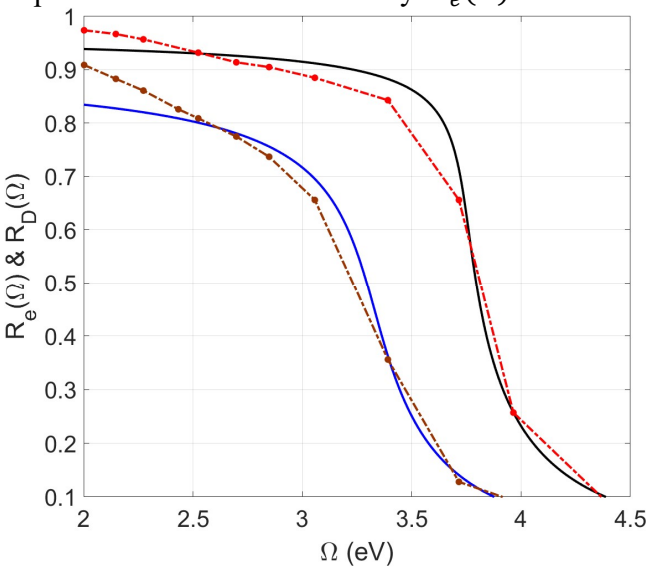

Fig. 16. Reflectance vs Ω for K and Rb. The dash-dot lines with points represent the experimental data $R_e(\Omega)$ from [17] while the full lines are for the outcome $R_D(\Omega)$ determined from the DM using parameters given in the text. The upper curves are for K and the lower ones for Rb.

graphs for potassium (K) and rubidium (Rb) reported by Monin and Boutry [17] in Fig. 16. The corresponding DM based results $R_D(\Omega)$ obtained by using $\omega_p = 3.75\,eV$, $\gamma = 0.1$ eV for K and $\omega_p = 3.32\,eV$, $\gamma = 0.24$ eV for Rb also constitute the content of this figure. The agreement between the model calculations and the experimental data for the two metals is reasonably good.

In contrast with alkali metals, optical properties of other metals like aluminium, silver, gold, copper, chromium, etc. are not explained by DM alone. These require DM combined with many-oscillator Lorentz model. As an example, we have considered aluminium (Al) because this can be safely considered as a free electron gas system

despite being a non-alkali metal. The experimental data for $n_e'(\Omega)$, $n_e''(\Omega)$, and $R_e(\Omega)$ for Ω up to 20 eV has been taken from [18] and plotted in Fig. 17. The presence of a peak in the first and dips in the last two at Ω close to 1.5 eV is quite clear. This is an

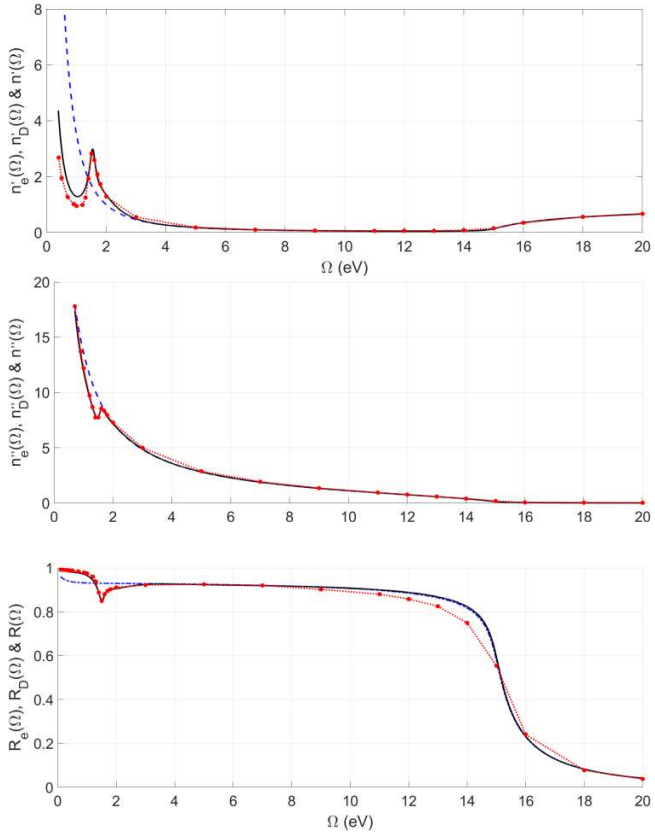

Fig. 17. Plots depicting experimental data $n_e'(\Omega)$, $n_e''(\Omega)$, and $R_e(\Omega)$ (red points joined with dot-dot line) [18]; DM fitting with $\omega_p = 15.0$ eV, $\gamma = 0.55$ eV (blue dash-dash line), and excellent DLOM fit obtained with four oscillators having parameters $\omega_p = 15.0\,eV$, $\gamma_0 = 0.04$ eV, $f_0 = 0.51$ (DM contribution), $\omega_{01} = 0.12$ eV, $\gamma_1 = 0.35$ eV, $f_1 = 0.23$, $\omega_{02} = 1.56$ eV, $\gamma_2 = 0.23$ eV, $f_2 = 0.04$, $\omega_{03} = 1.80$ eV, $\gamma_3 = 1.35$ eV, $f_3 = 0.19$, $\omega_{04} = 4.3$ eV, $\gamma_4 = 5.0$ eV, and $f_4 = 0.03$ (black solid line) for aluminium.

indication of departure from the DM behaviour, which too is shown in the figure; the parameters used to get this plot are $\omega_p = 15.0\,eV$, $\gamma =$ 0.55 eV. An impressive fit to the experimental data is obtained using DLOM with four oscillators with the parameters listed in the caption of Fig. 17; the relevant optical parameters have been denoted by $n'(\Omega)$, $n''$and $R(\Omega)$.

(iv). In ionic solids like sodium chloride, potassium chloride, rubidium bromide, etc. both cations and anions are charged and undergo vibrations about their equilibrium positions in the crystal lattice. As
such, these can be treated as Lorentz oscillators with equal and opposite charges, and mass that of the relevant ion. Obviously, masses of these oscillators are much higher, and their fundamental angular frequencies are much smaller as compared to the corresponding quantities for electronic oscillators considered in section 2. Generally, their resonant frequencies lie in the infrared region. In addition, the valence electrons of the cations as well as the anions can also be treated as Lorentz oscillators having high characteristic frequencies. Consequently, the dielectric and optical properties of these types of crystals get contributions from ionic as well as electronic oscillators and their experimental data have been analyzed using numerous-oscillators LOM. As an example, it may be mentioned that reflectance vs Ω plot for potassium chloride has about six sharp peaks with maximum value of about 0.3, and some broad peaks for Ω between 7 eV and 22 eV [3]. Obviously, its analysis will involve many Lorentz oscillators.

(v). A plasma is an electrically conducting medium having nearly equal number of positively charged ions and electrons, produced at high temperatures and / or very low number density. The ions and electrons can move around independently of each other. Since the electrons are not bound to any ion, like metals, a plasma does not have any characteristic resonant frequency, i.e., $\omega_0 = 0$. Furthermore, because of low number density (N) ω_p is quite small ($\sim 4 \times 10^{-5} - 4 \times 10^{-3}\,eV$) and the collisions of electrons are essentially negligible implying that $\gamma = 0$. Thus, a plasma essentially

corresponds to the first case discussed in Section 4. Accordingly, for a plasma $\varepsilon_r(\Omega) = 1 - \left(\omega_p/\Omega\right)^2$, which is a real quantity. Also, $n(\Omega) = \sqrt{1 - \left(\omega_p/\Omega\right)^2}$. Both of these are close to unity for very large Ω values. Note that $n(\Omega)$ is imaginary for $\Omega < \omega_p$ and real but less than unity for $\Omega > \omega_p$. Furthermore, from $\gamma = 0$ case in Fig.12, we infer that a plasma will be 100% reflective for e.m. waves of frequency $\Omega < \omega_p$ and highly transmissive for Ω significantly higher than ω_p. This is in consonance with the fact that ionosphere, which is a plasma layer around the earth having $\omega_p \sim 10^8$ rad s^{-1}, reflects back the radio signals of lower frequencies extending the range of receiving stations on the earth and is transparent to the signals with higher frequencies (the so-called short waves) enabling communication with satellites in space.

6 Epilogue

It is worth mentioning that at extremely high angular frequencies ($\Omega \to \infty$), the dielectric function is real and unity in LOM as well as DM. Physically, this means absence of polarization of the medium which is so because the electrons do not respond to the applied field. Under these conditions, there is neither refraction nor absorption and only high transmission of the incident e.m. wave.

We close the article by quoting Wooten [3], 'Both the Lorentz and Drude models are largely ad hoc, but still useful as starting points and for developing a feeling for optical properties. …many features of these classical models have quantum mechanical counterparts which are easily understood as generalizations of their classical analogs'.

Acknowledgement
The author is beholden to the learned referee for the thoughtful suggestions which have led to an overall improvement of the presentation of the article.

Appendix : Analysis of Complementary and Particular Integral Solutions for a One-dimensional Forced Oscillator

The equation of motion giving dynamical balance of forces for a one-dimensional forced damped harmonic oscillator corresponding to the one described by Eq. (1) can be written as

$$\ddot{x}(t) + \gamma\dot{x}(t) + \omega_0^2\, x(t) = Fe^{-i\Omega t}. \qquad \text{(A1)}$$

Here, $x(t)$ is instantaneous displacement, F is the amplitude of the applied force and other symbols have the same meaning as in Eq. (1). The general solution of this second-order nonhomogeneous linear differential equation with constant coefficients consists of two parts: (i) the complementary or homogeneous solution, $x_{CF}(t)$, and (ii) the particular or nonhomogeneous solution, which is also called particular integral, $x_{PI}(t)$. For an underdamped oscillator satisfying the condition $\gamma < 2\omega_0$, these solutions are given by

$$x_{CF}(t) = Ae^{-\gamma t/2} sin\,(\omega t + \theta) \qquad \text{(A2)}$$

with A as amplitude, $\omega = \omega_0\sqrt{1 - \frac{\gamma^2}{4\omega_0^2}}$ as damped angular frequency, and θ as initial phase; and

$$x_{PI}(t) = \frac{1}{(\omega_0^2 - \Omega^2) - i\gamma\Omega} Fe^{-i\Omega t}$$

$$= \left\{\frac{(\omega_0^2 - \Omega^2) + i\,\gamma\Omega}{(\omega_0^2 - \Omega^2)^2 + (\gamma\Omega)^2}\right\} Fe^{-i\Omega t}. \qquad \text{(A3)}$$

Accordingly, for the complete solution of Eq. (A1), we have

$$x(t) = x_{CF}(t) + x_{PI}(t). \qquad \text{(A4)}$$

Note that for an oscillator having initial displacement x_0 and initial velocity v_0,

$$A = \frac{\sqrt{\omega^2 x_0^2 + (v_0 + \frac{\gamma x_0}{2})^2}}{\omega}, \quad \text{and} \quad \theta = tan^{-1}\left(\frac{\omega x_0}{v_0 + \frac{\gamma x_0}{2}}\right). \tag{A5}$$

Also, in Eq. (A2), since $e^{-\frac{\gamma t}{2}}$ is a uniformly decreasing function of time, $x_{CF}(t)$ describes oscillations about the equilibrium position with continuously diminishing amplitude $Ae^{-\frac{\gamma t}{2}}$ till it becomes zero. Note that the oscillations $x_{CF}(t)$ are usually referred to as transients and effective or damped amplitude $Ae^{-\frac{\gamma t}{2}}$ is said to define the envelope of decay of $x_{CF}(t)$. Obviously, the decrease in amplitude is fast if γ is large and vice versa. To appreciate the effect of damping parameter γ on $x_{CF}(t)$ in a better way, we note that $Ae^{-\frac{\gamma t}{2}}$ will be 0.1 % of A at time $T = \frac{-2 \ln (0.001)}{\gamma} = \frac{13.82}{\gamma}$. Thus, for $t > T$, $Ae^{-\frac{\gamma t}{2}}$ and hence $x_{CF}(t)$ may be essentially taken as zero.

Next, simplifying Eq. (A3), we can write its real part as

$$x'_{PI}(t) = B\cos(\Omega t - \varphi), \tag{A6}$$

where

$$B = \frac{F}{\sqrt{\left(\omega_0^2 - \Omega^2\right)^2 + (\gamma\Omega)^2}}, \text{ and } \varphi = tan^{-1}\left(\frac{\gamma\Omega}{\omega_0^2 - \Omega^2}\right). \tag{A7}$$

In fact, this is the same expression as we obtain by considering the nonhomogeneous term as $F\cos(\Omega t)$ in Eq. (A1). Clearly, $x'_{PI}(t)$ is an oscillatory function with constant amplitude B.

From experimental observation point of view, a complete solution for Eq. (1) can be written as

$$x(t) = x_{CF}(t) + x'_{PI}(t). \tag{A8}$$

As argued above, for sufficiently large times $t > T$, the transients vanish and only the particular solution is left, and we have

$$x(t) = x'_{PI}(t). \tag{A9}$$

This is said to give a steady state solution to the problem.

To elaborate this aspect in a proper perspective, we have plotted $x_{CF}(t)$, $x'_{PI}(t)$, and $x(t) = x_{CF}(t) + x'_{PI}(t)$ for a damped forced oscillator characterized by (arbitrarily chosen) parameters ω_0 = 4.0 rads^{-1}, γ = 1.0 s^{-1}, x_0 = 0.03 m, v_0 = 0.50

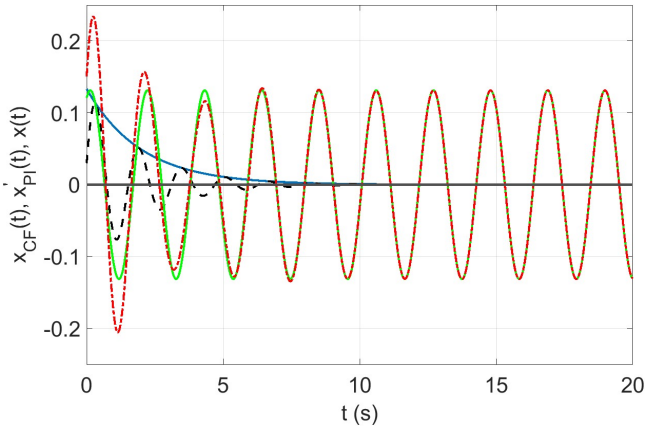

Fig. A1. Plots showing time variation of $x_{CF}(t)$ (black dashed line), $x'_{PI}(t)$ (green solid line), and $x(t)$ (red dash-dot line) for a forced oscillator having parameter values listed in the text. Blue solid line represents the envelope of decay of $x_{CF}(t)$.

ms^{-1}, F = 1.0 N, and Ω = 3.0 rads^{-1} so that ω = 3.97 rads^{-1}, A = 0.13 m, θ = 0.23 rad, B = 0.13 m, and φ = 0.40 rad, in Fig. A1. This clearly shows that for small t values $x(t)$ gets contribution from both $x_{CF}(t)$ and $x'_{PI}(t)$, while for reasonably large times $(t > T = 13.82\ s)$ $x_{CF}(t) = 0$ and $x(t) = x'_{PI}(t)$, the steady state solution. We can extend this treatment straightaway for a forced one-dimensional harmonic oscillator to the case of relevant three-dimensional oscillator.

References

[1] The Nobel Foundation, *Nobel Lectures - Physics 1901-1921,* (Elsevier, Amsterdam, 1967).
[2] H. A. Lorentz, Proc. Koninklijke Akademie van Wetenschappen (Netherlands) **8**, 591 (1906).
[3] F. Wooten, *Optical Properties of Solids,* (Academic Press, New York, 1972).
[4] I. F. Almog, M.S. Bradley, and V. Bulovic, The Lorentz Oscillator and its Applications, https://ocw.mit.edu>resources>mit6_007s11_ lorentz (2011).
[5] A. Zangwill, *Modern Electrodynamics*, (Cambridge University Press, Cambridge, 2012).
[6] M. J. Mageto, C. M. Maghanga, and M. Mwamburi, Afr. Rev. Phys. **7:0011,** 95 (2012).
[7] D. J. Griffiths, *Introduction to Electrodynamics*, (Pearson, London, 2013).
[8] P. Hofmann, *Solid State Physics: An Introduction,* (Wiley-VCH, Weinheim, 2015).
[9] R. C. Rumpf, *Electromagnetic Properties of Materials – Lorentz and Drude Models, https://*empossible.net/wp-content/uploads/2018/ 03/Lecture-2-Lorentz-and-Drude-models.pdf (2016)
[10] D. Marasinghe, *Drude-Lorentz Analysis of the Optical Properties of the Quasi-two-Dimensional Dichalcogenides 2H-$NbSe_2$ and 2H-$TaSe_2$*, https://etd.ohiolink.edu›rws_etd›send_file›send (2018).
[11] Ph. W. Courteille, *Electrodynamics*, https://www.ifsc.usp.br ›ElectroDynamicsScript (2021).
[12] J. S. Colton, Lorentz Oscillator Model, http://www.physics.byu›docs›phy442-summer21 (2021).
[13] J. Zhu, J. Zhang, Y. Li, and others, AIP Advances **5**, 117217 (2015).
[14] J. Zhang, K. Li, Z. Fang, and others, AIP Advances **11**, 075218 (2021).
[15] A. R. Forouhi and I. Bloomer, J. Phys. Common. **5**, 025002 (2021).
[16] http://www.filmetrics.com/refractive index data base.
[17] J. Monin and G. A. Boutry, Phys. Rev. B **9**, 1309 (1974).
[18] H. J. Hagemann, W. Gudat, and C. Kunz, DESY SR-74 / 7 (1974).